

Supplementary Information

Nanotubular structured Si-based multicomponent anodes for high-performance lithium-ion batteries with controllable pore size via coaxial electrospinning

By *Jaegeon Ryu, Sinho Choi, Taesoo Bok, and Soojin Park**

Department of Energy Engineering, School of Energy and Chemical Engineering, Ulsan National Institute of Science and Technology (UNIST), UNIST-gil 50, Ulsan 689-798, Republic of Korea

Table S1. Electrochemical properties of Si-based anode materials

Structure	Synthetic methods	First charge capacity (mAh/g)	Capacity retention (%)	C-rate	Loading mass of active material (mg/cm ²)	Ref.
Si nanoparticle	Commercial	~2500	65 (400 cycles)	0.5 C	0.2-0.3	<i>Adv. Mater.</i> , 2013, 25 , 1571.
Porous Si	Mg reduction	~1650	62.6 (1000 cycles)	0.5 C	0.5-1.0	<i>Sci. Rep.</i> , 2014, 4 , 5623.
Si hollow sphere	Template etching	~2720	52.1 (700 cycles)	0.5 C	0.1-0.2	<i>Nano Lett.</i> , 2011, 11 , 2949.
Si-C yolk-shell	Carbon coating on Si-SiO ₂ core-shell and etching	1180	98.3 (1000 cycles)	0.5 C	0.2	<i>Nat. Nanotechnol.</i> , 2014, 9 , 187.
	Air inflation	1650	65 (40 cycles)	0.5 C	N/A	<i>RSC Adv.</i> , 2014, 4 , 36218.
Si nanowire	Template-based impregnation	~3000	33.5 (1000 cycles)	0.5 C	0.03-0.04	<i>Nano Lett.</i> , 2013, 13 , 5740.
Si nanotube	Mg reduction of SiO ₂ nanotubes	~1850	48.6 (90 cycles)	0.1 C	N/A	<i>Adv. Mater.</i> , 2012, 24 , 5452.
Ti_xSi_y-coated Si/Al₂O₃ nanotube	Coaxial-electrospinning and Al reduction	1540	75 (280 cycles)	0.5 C	1.59	This work

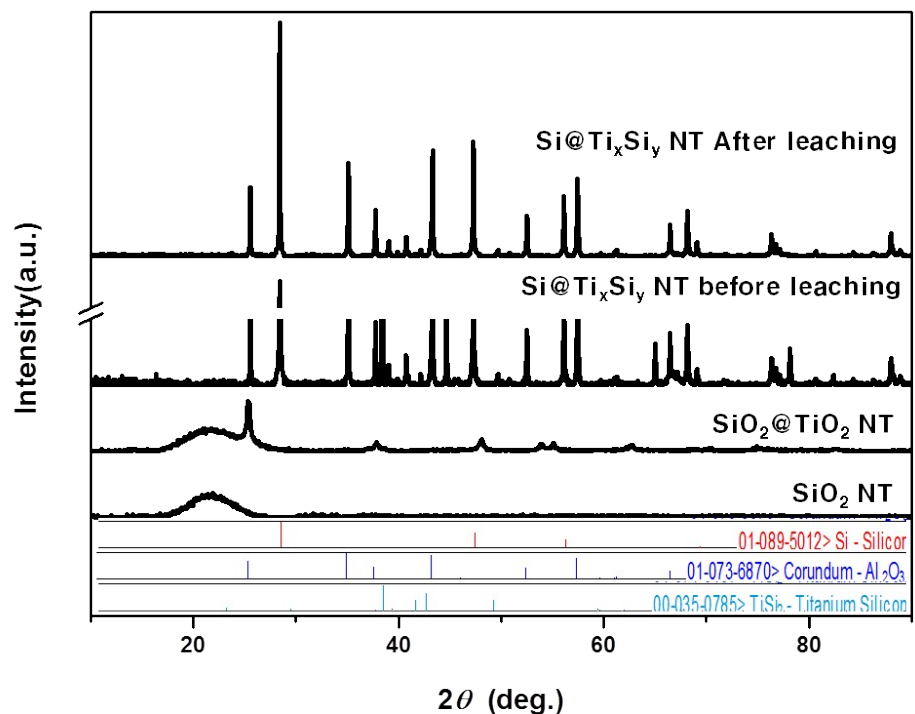


Fig. S1. XRD patterns of four types of tubular structures fabricated by co-axial electrospinning and/or aluminothermic reaction.

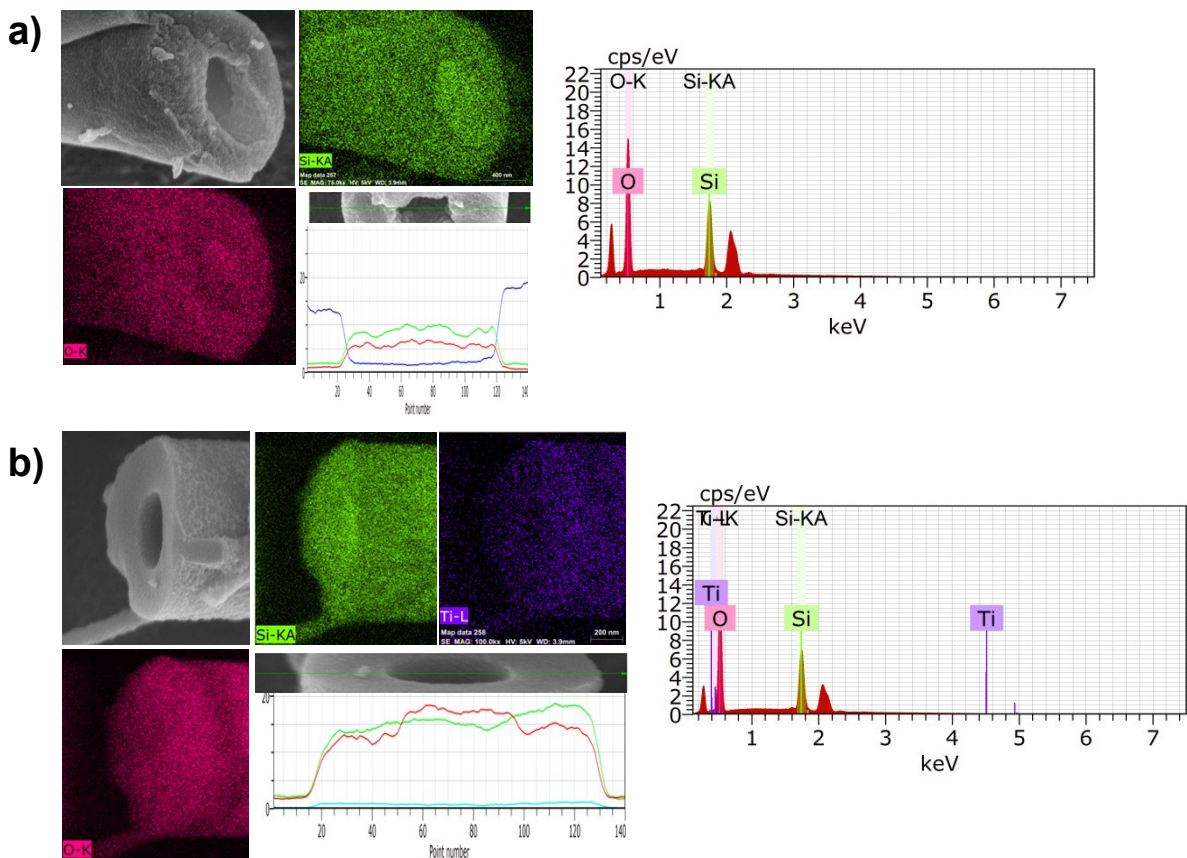


Fig. S2. EDS mapping and line scan spectrum of (a) SiO_2 nanotubes and (b) $\text{SiO}_2@\text{TiO}_2$ nanotubes.

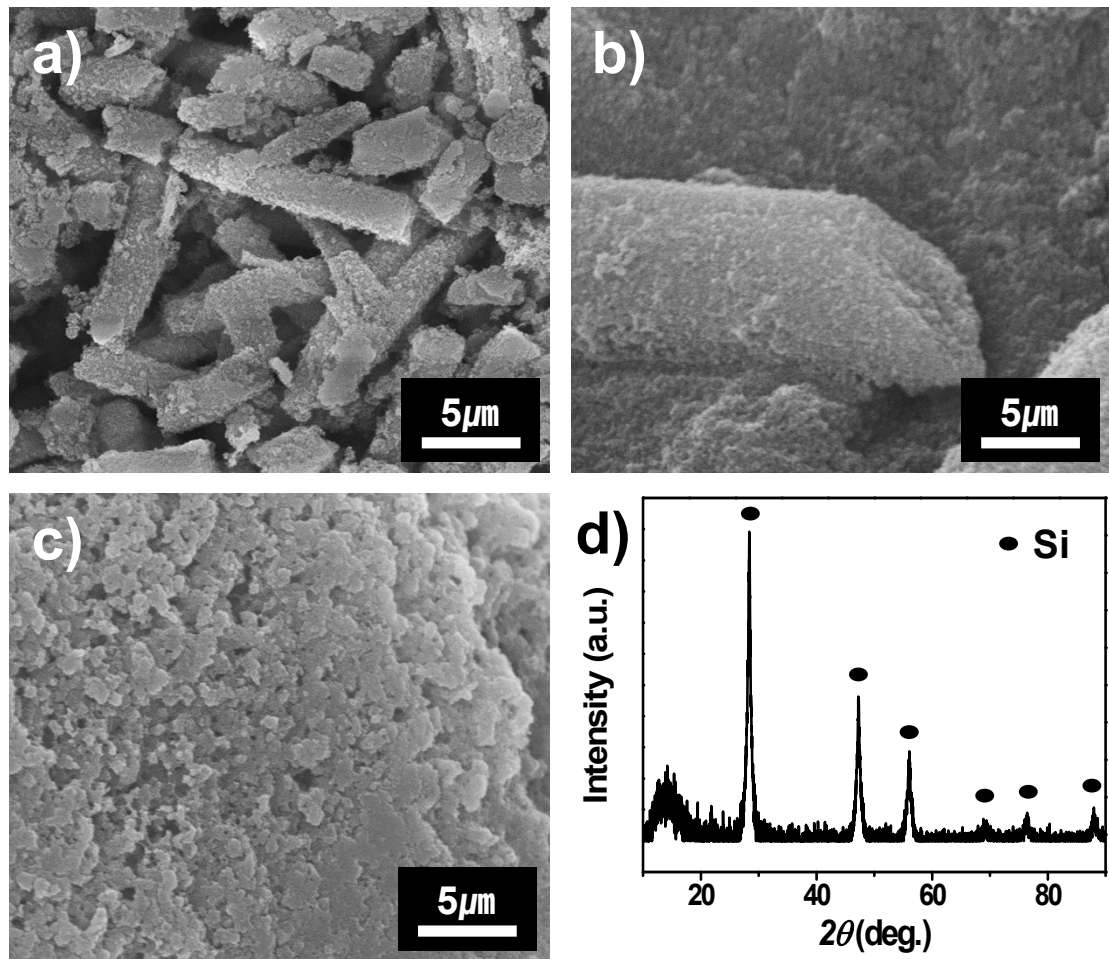


Fig. S3. Si nanotubes prepared by Mg reduction of SiO_2 nanotubes. (a-c) SEM images showing collapsed Si nanotube. (d) XRD pattern of collapsed Si nanotube obtained by magnesiothermic reaction.

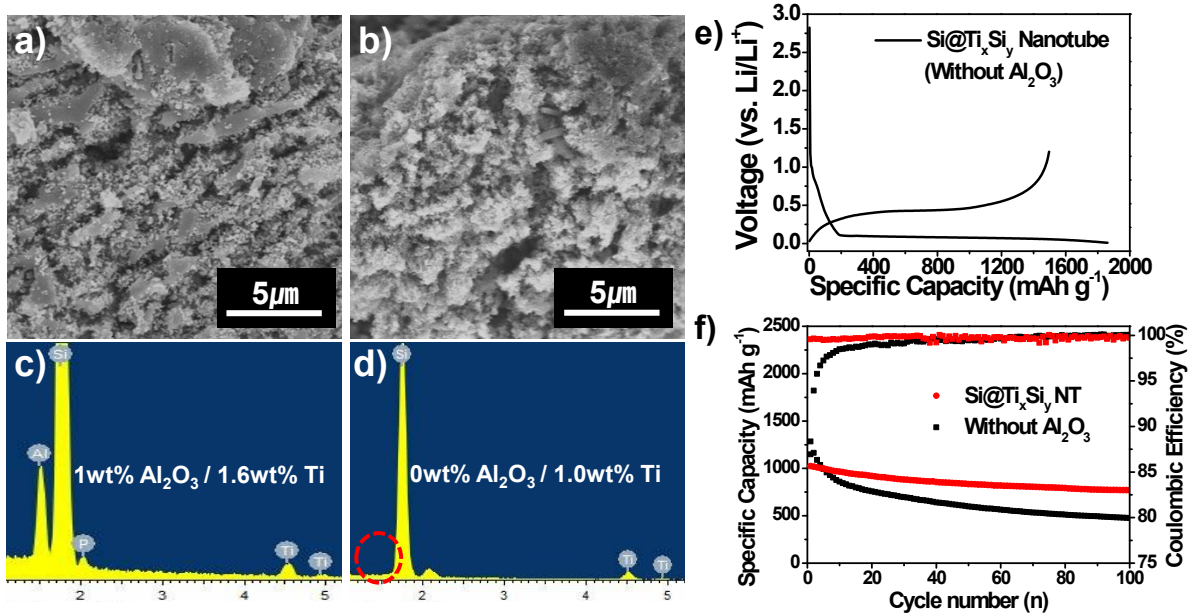


Fig. S4. SEM images of Ti_xSi_y-coated Si nanotubes after etching process with concentrated phosphoric acid at 150 °C for (a) 2 h (b) 3 h. (c) and (d) are EDS spectra of the corresponding SEM images of (a) and (b), respectively. (e) Voltage profile of formation cycle and (f) cycling retention of Si@Ti_xSi_y nanotubes without Al₂O₃ layer obtained at 0.5 C rate.

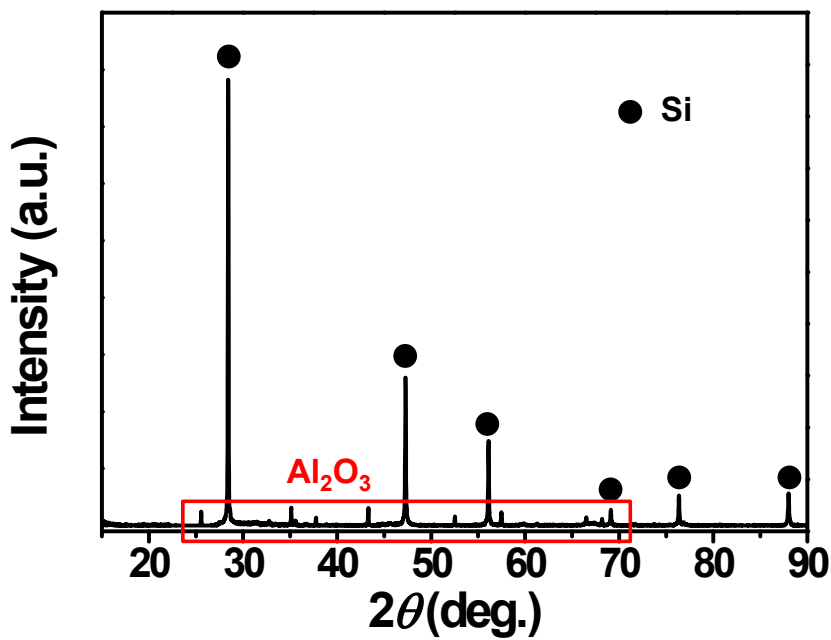


Fig. S5. XRD pattern of bare Si nanotubes prepared by aluminothermic reduction of SiO_2 nanotubes (without TiO_2 coating). During the aluminothermic reaction, both Si and Al_2O_3 were simultaneous formed after phosphoric acid leaching process

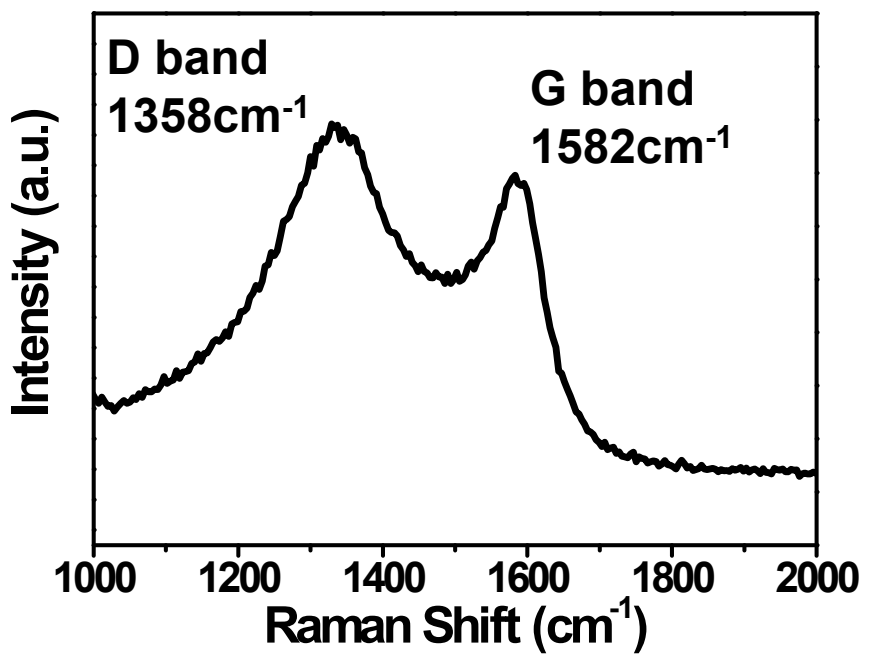


Fig. S6. Raman spectrum of carbon-coated Si nanotubes

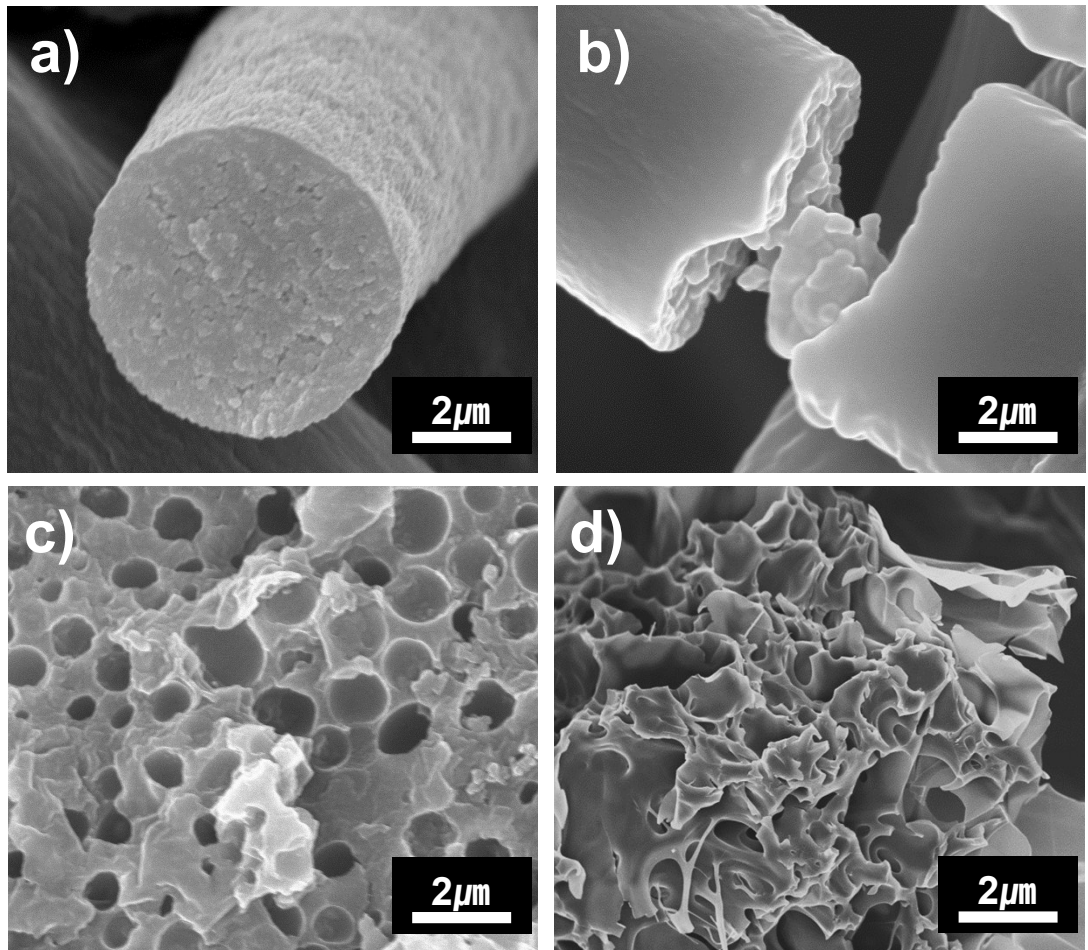


Fig. S7. SEM images of SiO_2 tubes fabricated by co-axial electrospinning process. (a) SiO_2 fiber fabricated at oil feeding rate of $0.01 \mu\text{L min}^{-1}$. (b) SiO_2 fiber with residual heavy oil in the central region of broken fibers. (c-d) SEM images showing collapsed SiO_2 fibers prepared at oil feeding rate of $10 \mu\text{L min}^{-1}$.

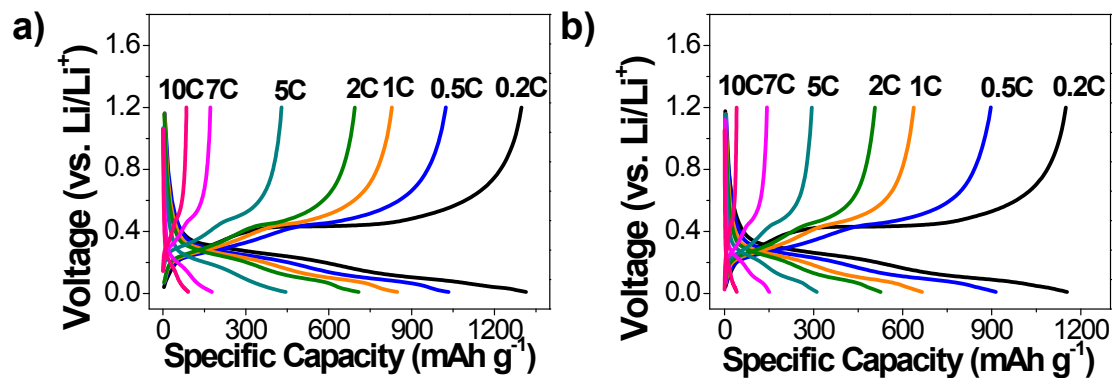


Fig. S8 Rate capabilities of (a) bare and (b) carbon-coated Si nanotubes at various C rates. The discharge and charge rates are the same.

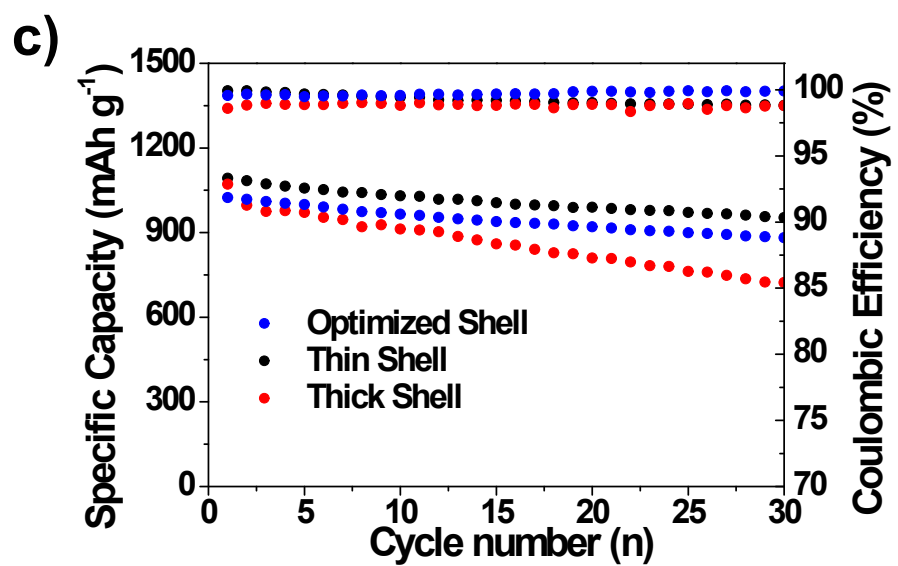
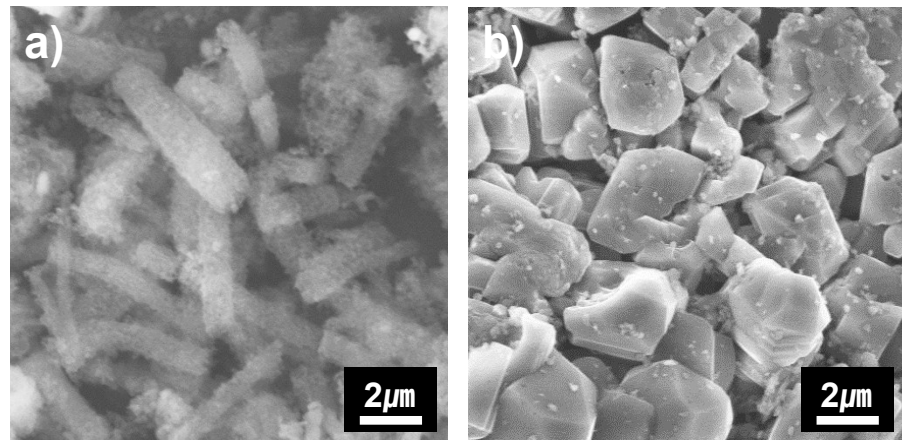


Fig. S9 SEM images of TixSiy -coated Si nanotubes with (a) thin-shell (100-200 nm) and (b) thick-shell (700-800 nm). (c) Cycling retention of three different Si-based electrodes obtained in the range of 0.01-1.2 V at 0.5 C rate.

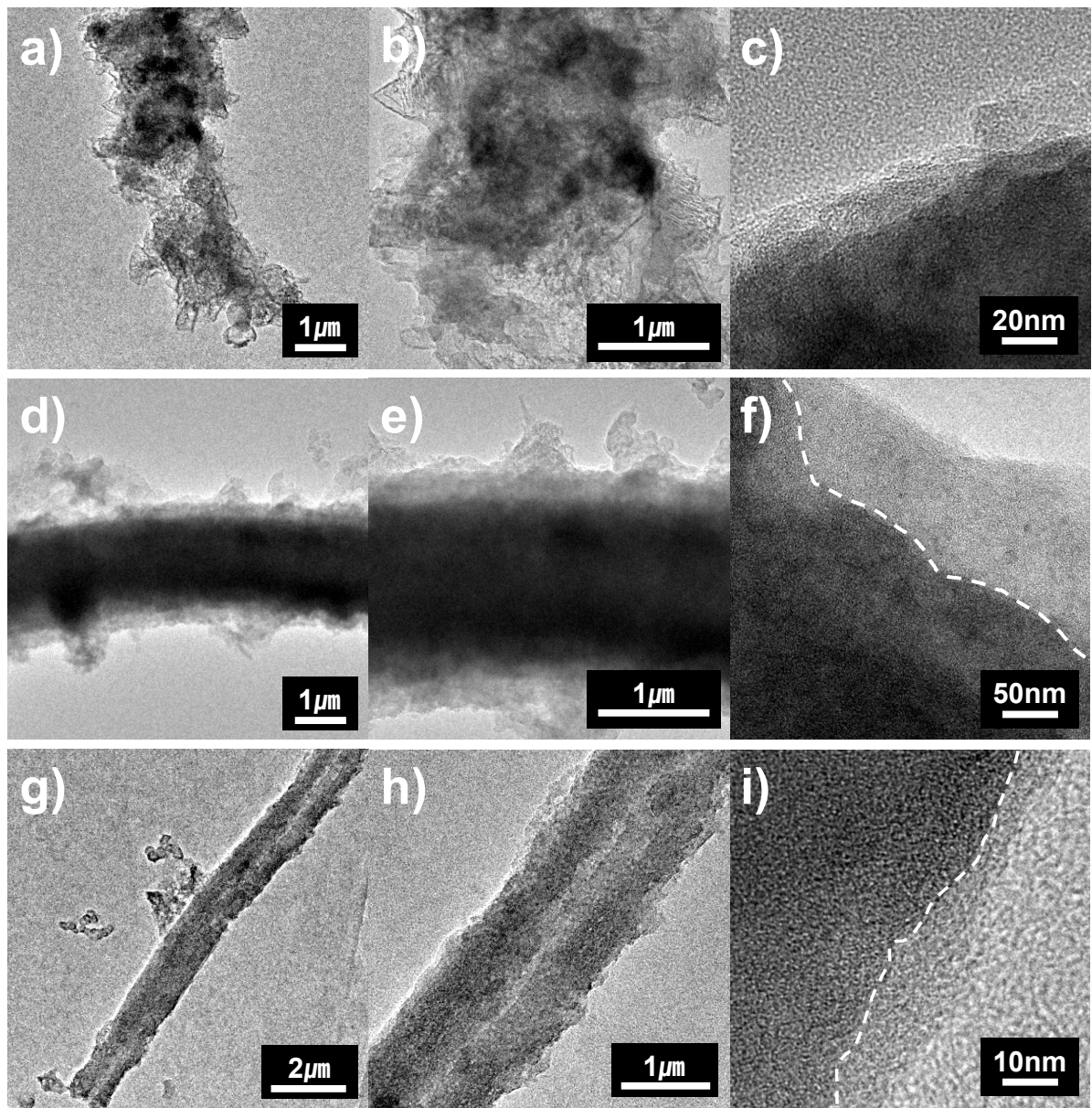


Fig. S10. TEM images of (a-c) bare, (d-f) carbon-coated, and (g-i) Ti_xSi_y -coated Si nanotubes at 0.5 C rate after 100 cycles.